

Phase transitions in the mesoscopic superconducting square

J. Bonča¹ and V. V. Kabanov²

¹*J. Stefan Institute 1001, Ljubljana, Slovenia*

²*FMF, University of Ljubljana, Ljubljana, Slovenia*

(Received 2 October 2001; published 12 December 2001)

We solve the Ginzburg-Landau equation for a mesoscopic thin film of square shape in the magnetic field. In the limit of large screening length we find a series of first- and second-order phase transitions as temperature and/or magnetic field changes. First-order phase transitions between giant-flux states can be described with a simple variational procedure. We discuss the similarity with rotating liquid He⁴ and derive a simple formula for H_{c1} . We identify order parameters based on symmetry arguments and we propose a Landau functional describing the second-order phase transition.

DOI: 10.1103/PhysRevB.65.012509

PACS number(s): 74.60.Ec, 74.25.Ha, 74.80.-g

Advances in nanotechnology and constantly shrinking semiconductor devices have motivated researchers to study properties of mesoscopic superconducting samples. One line of research in this field has focused on the problem of phase transitions in a mesoscopic superconducting sample under the influence of the external magnetic field.¹ There are two characteristic limits in which phase transitions have different properties. If the size of the sample $a \gg \xi$, where ξ is the superconducting coherence length, and the applied field is large enough, there are many vortices in the sample. In this case long-range interaction between vortices and image vortices is screened by spontaneous creation of vortex loops near the sample boundary² which leads to a decrease of the surface barrier for the vortex to penetrate the sample. In the opposite case, when $a \sim \xi \ll \lambda_{eff} = \lambda^2/d$, with λ being the London penetration depth and d being the thickness of the sample, there are only few vortices in the sample. The standard Abrikosov approach³ must be modified because of the strong influence of the sample boundaries. In this case magnetic field is uniform throughout the sample. The thermodynamics of this system is determined by the repulsion between vortices and Bean-Livingston barrier forces⁴ on the scale $r \sim \xi$.

Different approaches have been applied for the investigation of phase transitions in the latter limit. Most of them consider disk geometry. Buzdin and Brison applied electrostatic formalism to consider influence of the barrier on the vortex structure of a thin superconducting disk.⁵ Within this approach vortices are replaced by the hard-core particles interacting through Coulomb forces. Numerical solution of the Ginzburg-Landau equation (GLE) for the same geometry reveals a series of the first and second order phase transitions in the superconducting disk. Such transitions take place between giant vortex states with different vorticity as well as between a giant vortex state and a multivortex state as the external field changes.⁶⁻⁸ We emphasize an important difference between the disk and the square geometries. Solution of the linearized GLE, describing the nucleation of the superconducting order parameter near the H_{c2} line for the disk, always corresponds to the giant vortex state. On the other hand, as it was demonstrated by Chibotaru *et al.*,¹ there are many well-separated zeros of the order parameter in the case of the square sample. Consequently, the behavior of the

square sample near the H_{c2} line should be qualitatively different from the disks. On the basis of the solution of the linearized GLE the appearance of the antivortex in the center of the sample has been predicted.¹

In this paper we investigate phase transitions in a superconducting film of square shape as a function of temperature T and external magnetic field H in the limit $a \sim \xi \ll \lambda_{eff}$. We solve the GLE for thin superconducting films with thickness $d \ll \lambda$. Our results are also valid for a type-two superconducting cylinder of square cross section, if the Ginzburg-Landau parameter $\kappa = \lambda/\xi \gg 1$. We show that a configuration with one antivortex in the center and four vortices on the diagonals of the square is unstable when we move away from the H_{c2} line and the nonlinear term in the GLE is considered. On the contrary, at higher magnetic field, the configuration with four vortices on diagonals of the square remains stable. Similar to the superconducting disk⁶⁻⁸ we find a sequence of phase transitions of the first order between giant vortex states as well as between multivortex states with different vorticity. Second-order phase transition takes place when a giant vortex state splits into a multivortex state while simultaneously breaking the C_4 symmetry. Such transitions are discussed in terms of the phenomenological theory of Landau.

The GLE for dimensionless order parameter ψ has the form

$$\xi^2 \left(i\nabla + \frac{2\pi\mathbf{A}}{\Phi_0} \right)^2 \psi - \psi + \psi|\psi|^2 = 0. \quad (1)$$

here $\xi = (\hbar^2/4m|\alpha|)$, α is the temperature-dependent parameter of the Ginzburg-Landau expansion for the free energy, Φ_0 is the flux quantum, and \mathbf{A} is the vector potential $\mathbf{H} = \nabla \times \mathbf{A}$. The second GLE equation for the vector potential can be written as

$$\nabla \times \nabla \times \mathbf{A} = -i \frac{\Phi_0}{4\pi\lambda^2} (\psi^* \nabla \psi - \psi \nabla \psi^*) - \frac{|\psi|^2 \mathbf{A}}{\lambda^2}. \quad (2)$$

Since we consider the case of a small mesoscopic square where $a \sim \xi \ll \lambda_{eff}$, the magnetic field is uniform in the film. The correction to the external field is of the order of $1/\kappa^2$ and may be found by solving Eq. (1) while assuming uniform magnetic field and substituting the solution of Eq. (1) into

Eq. (2). Such a solution is equivalent to the expansion of the free energy in a $d/\lambda\kappa$ series. In addition to Eq. (1) we have to supply the boundary condition for the superconductor-insulator junction:

$$\left(i\nabla + \frac{2\pi\mathbf{A}}{\Phi_0}\right) \cdot \mathbf{n}\psi = 0, \quad (3)$$

where \mathbf{n} is a normal vector to the surface of the sample.

Introducing $N \times N$ discrete points in the square we rewrite Eq. (1) in the form of a nonlinear discrete Schrödinger equation:

$$\sum_{\mathbf{l}} t_{\mathbf{l}+\mathbf{i},\mathbf{i}}\psi_{\mathbf{l}+\mathbf{i}} - 4t_{\mathbf{i},\mathbf{i}}\psi_{\mathbf{i}} - \psi_{\mathbf{i}} + \psi_{\mathbf{i}}|\psi_{\mathbf{i}}|^2 = 0, \quad (4)$$

where the summation index $\mathbf{l} = (\pm 1, 0), (0, \pm 1)$ points toward nearest neighbors, and $t_{\mathbf{l},\mathbf{i}} = (\xi N/a)^2 \exp[-(2\pi i/\Phi_0) \int_{\mathbf{i}}^{\mathbf{l}} \mathbf{A}(\mathbf{r}) d\mathbf{r}]$.⁹ Equivalent discretization of the boundary conditions, Eq. (3), provides an additional equation which can be directly solved and substituted into Eq. (4). As a result, equations close to the boundary are slightly different from the ‘‘bulk.’’

$$\sum_{\mathbf{l}} t_{\mathbf{l}+\mathbf{i},\mathbf{i}}\psi_{\mathbf{l}+\mathbf{i}} - \epsilon(\mathbf{i})t_{\mathbf{i},\mathbf{i}}\psi_{\mathbf{i}} - \psi_{\mathbf{i}} + \psi_{\mathbf{i}}|\psi_{\mathbf{i}}|^2 = 0, \quad (5)$$

where $\psi_{\mathbf{i}} = 0$ if \mathbf{i} is outside the sample, $\epsilon(\mathbf{i}) = 4 - \delta_{i_x,1} - \delta_{i_x,N} - \delta_{i_y,1} - \delta_{i_y,N}$, and $\mathbf{i} = (i_x = 1, \dots, N, i_y = 1, \dots, N)$. There is one important advantage of such a treatment of the boundary condition. When neglecting the nonlinear term in Eq. (4), the system of linear equations reduces to the problem of eigenvalues and eigenfunctions of the Hermitian matrix. On the other hand, the solution of nonlinear equations requires iterations and inversion of the Hermitian matrix.

Let us first discuss the solution of the linearized GLE and compare our results with previous studies.¹ The lowest eigenvalue of the linear GLE determines the upper critical field of the sample. We have calculated eigenvalues of the linear problem expressed in units $[a/\xi(T)]^2$ as a function of the dimensionless external magnetic field $h = \Phi/\Phi_0$ where Φ is the total flux through the sample. Our results for a few lowest eigenvalues agree within the linewidth with the results of Ref. 1. The spatial pattern of the order parameter is also similar. For the field $h \approx 5.5$ we have observed five zeros of the order parameter near the center of the square. The solution corresponds to four vortices on the diagonals and one antivortex in the center of the square with total vorticity $m = 3$.¹ The distance between vortices is of the order of $\delta \approx 0.12\xi \ll \xi$. The maximum value of the order parameter $|\psi(x,y)|$ in the region between zeros is small (four orders less than the value of the order parameter near the sample boundary). This indicates that the vortex-anti-vortex structure becomes unstable when we move away from the H_{c2} line, and the nonlinear term and $1/\kappa$ corrections are considered. Moreover, the screening currents flowing between zeros are small. In that case correction to the external field is determined by the current flowing near the sample bound-

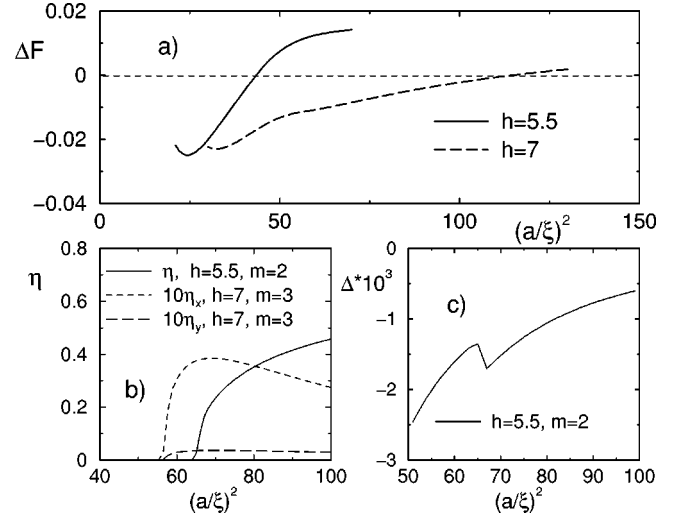


FIG. 1. (a) Difference in the free energy ΔF in units of $[\Phi_0^2 a^2 d / (4\pi)^3 \lambda^2 \xi^2]$ between solutions with different integral vorticities. For the case of $h = 5.5$, $\Delta F = F(m=3) - F(m=2)$ and for $h = 7$, $\Delta F = F(m=4) - F(m=3)$. (b) Order parameter η vs $(a/\xi)^2$ for the solution with $m=2$ calculated at $h=5.5$, and the two-dimensional order parameters η_x and η_y for the solution with $m=3$ calculated at $h=7$. (c) The second derivative of the free energy $\Delta = d^2 F / d[(a/\xi)^2]^2$ for the solution with $m=2$ at $h=5.5$.

aries. Consequently, we do not expect suppression of the field in the core of the antivortex.

In the following we consider the changes in the vortex structure when we move away from the H_{c2} line. Taking into account the nonlinear term, we were unable to detect more than one zero of the order parameter near the origin of the square for the value of the field $h = 5.5$. Consequently, the solution with more than one zero survives only very close to the H_{c2} line. These findings are supported by a recent work by Baelus and Peeters.¹⁰ We do not expect any phase transition at the point where all zeros are joined together since total flux and the symmetry of the solution do not change. This situation is different from the case of the higher field $h = 7$, where the solution with four zeros of the order parameter survives far from the H_{c2} line. In fact, the giant-flux solution was not detected in that case.

In Fig. 1(a) we plot the difference in the free energy between solutions with different integral vorticity $\Delta F = F(m=3) - F(m=2)$ as a function of $(a/\xi)^2$ for the fixed magnetic field $h = 5.5$. As is clearly seen from the figure, near $(a/\xi)^2 \approx 43$, a first-order phase transition takes place. At that point the high-temperature phase corresponding to the giant vortex with $m=3$ becomes metastable, and the phase corresponding to giant vortex, shown in Fig. 2 (left), with $m=2$ becomes a ground state. At this point, the slope of the first derivative of the free energy as a function of T is discontinuous, which corresponds to the latent heat of the transition. With further decrease of the temperature and ξ , the second transition takes place. At $(a/\xi)^2 \sim 66$ the giant vortex located in the center splits along one of the diagonals, Fig. 2 (right). This transition is the second order phase transition, where $|\psi|^2$ is no longer invariant under the fourfold axis of the

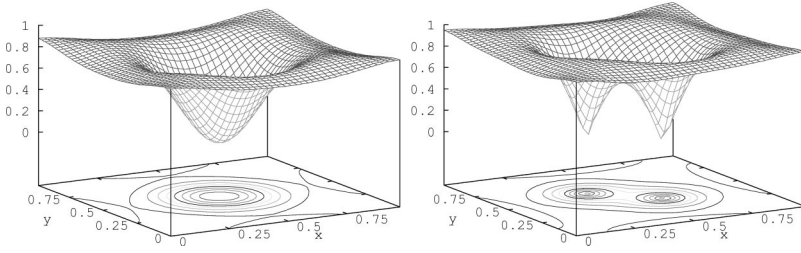


FIG. 2. $|\psi(x,y)|$ calculated at a fixed magnetic field $h=5.5$. Presented are solutions with lowest free energy calculated at $(a/\xi)^2=50$ with one giant flux $m=2$ (left) and $(a/\xi)^2=90$ with two separated fluxes each carrying $m=1$ (right). Contours represent $|\psi(x,y)|=0.1, \dots, 0.9$.

square. The phase transition is clearly observed by computing the order parameter $\eta = \int xy |\psi(x,y)|^2 dx dy$, presented in Fig. 1(b). A nonvanishing η is followed by a jump in the second derivative of the free energy $\Delta = d^2 F/d[(a/\xi)^2]^2$, presented in Fig. 1(c). We estimated the magnitude of the effect in terms of the specific-heat jump: $\Delta C/a^2 d = [5 \times 10^{-3} \Phi_0^2 T'_c / (4\pi)^3 \lambda^2 \xi^2 T_c^2]$, where T'_c is the critical temperature of the transition determined by the condition $(a/\xi)^2 \approx 66$, and T_c is the critical temperature of the sample at $h=0$. The Landau functional, describing this phase transition, is defined as $F = \alpha_1 \eta^2 + \beta_1 \eta^4$, where α_1 and β_1 are Landau coefficients with $\alpha_1 \propto (T - T'_c)$. This phase transition corresponds to the one-dimensional corepresentation B of the nonunitary $C_{4v}(C_4)$ group.

Since we restrict our calculation to the case $\lambda_{eff} \gg a \sim \xi$ long-range forces between vortices are irrelevant. At short distances $r \sim \xi$ interaction between vortices is different from that in the London limit because of substantial overlap of the vortex core. The interaction with the boundaries is determined by the Bean-Livingston barrier,⁴ interaction of the vortex with the screening current, which is the strongest near sample boundaries, and interaction caused by the overlap of the vortex core with the boundaries. For the field $h=5.5$ in the vicinity of the H_{c2} line the interaction with the boundaries is larger than the repulsion between vortices and the giant vortex with $m=3$ is located in the center of the sample. With the decrease of ξ the energy difference between two different solutions with different vorticity decreases and the first order phase transition to a giant-flux state with vorticity $m=2$ takes place at $(a/\xi)^2 \approx 43$. A giant-flux state (with lower vorticity) remains stable, since the interaction with the sample boundaries still dominates over the repulsion between vortices. Further decrease of ξ leads to the decrease of the interaction of the vortices with the boundaries, and repulsion between vortices in the giant-flux state starts to dominate. As a result a second-order phase transition [at $(a/\xi)^2 \approx 66$] between the giant vortex state and the multivortex state takes place, preserving the integral vorticity. Separation

between vortices is determined by the vortex-vortex repulsion that tends to separate them as far as possible, while to the contrary, repulsion from the boundaries prevents vortices from approaching the boundaries.

The situation is different when the external magnetic field is increased to $h \approx 7$. In that case near the H_{c2} line the ground state corresponds to a multivortex state with the total vorticity $m=4$, Fig. 3 (left). When temperature decreases, the first-order phase transition takes place at $(a/\xi)^2 = 110$, see Fig. 1(a). At this point the multivortex state with $m=4$ becomes unstable while the multivortex state with $m=3$, presented in Fig. 3 (right), represents the solution with the lowest free energy. Apart from the change of the vorticity, the symmetry is also reduced at the transition point. A phase transition takes place in accordance with joint corepresentation E^\pm of the nonunitary group $C_{4v}(C_4)$. Consequently, four orientations of the pseudodipolar moment of the vortices are possible. The two-component order parameter corresponding to a given change of symmetry, presented in Fig. 1(b), can be determined as follows: $\eta_x = \int x |\psi(x,y)|^2 dx dy$, $\eta_y = \int y |\psi(x,y)|^2 dx dy$. Free energy in that case depends on the vorticity m and order parameter η_x, η_y . $F(m = 4, \eta_x, \eta_y)$ always has a minimum at $\eta_x = \eta_y = 0$. For $m=3$, $F(m=3, \eta_x, \eta_y) = \alpha_2(\eta_x^2 + \eta_y^2) + \beta_2(\eta_x^4 + \eta_y^4) + \gamma_2 \eta_x^2 \eta_y^2$, where $\alpha_2, \beta_2, \gamma_2$ are Landau coefficients, and $\alpha_2 \propto (T - T'_c)$, where T'_c is the temperature of the transition between the giant vortex state and the multivortex state for the case $m=3$. T'_c is determined by the condition $(a/\xi)^2 \approx 56$. This transition is unobservable because T'_c is lower than the transition temperature for the first-order phase transition where the vorticity m changes from $m=3$ to $m=2$ [compare Figs. 1(a) and 1(b)].

The first-order phase transition between giant vortex states with different vorticity can be described qualitatively on the basis of a simple variational function for the order parameter. Spatial dependence of the order parameter in the giant vortex state with vorticity m can be approximated by the function

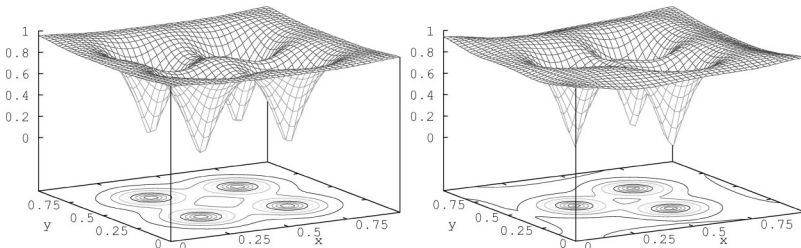


FIG. 3. $|\psi(x,y)|$ calculated at a fixed magnetic field $h=7$. Presented are solutions with lowest free energy calculated at $(a/\xi)^2=100$ (left) and $(a/\xi)^2=120$ (right). Contours are defined as in Fig. 2.

$$\psi(r, \phi) = \begin{cases} (r/\xi)^m \exp(im\phi) & r < \xi, \\ \exp(im\phi) & r > \xi. \end{cases} \quad (6)$$

Substituting this function into the Ginzburg-Landau functional and keeping only leading terms in $(a/\xi)^2$, we obtain a simple expression for the free energy:

$$F \simeq \frac{\Phi_0^2 d}{(8\pi)^2 \lambda^2} [m^2 \ln(a^2/\pi\xi^2)/2 - \Phi \cdot m/\Phi_0]. \quad (7)$$

Minimization of Eq. (7) in the large $m \gg 1$ limit provides the expression for the vorticity:

$$m \simeq \frac{\Phi}{\Phi_0} / \ln(a^2/\pi\xi^2). \quad (8)$$

Minimization of Eq. (7) at $h=5.5$ leads to the estimated value for the phase transition from $m=3$ to $m=2$ at $(a/\xi)^2=28$, which is lower than the calculated value $(a/\xi)^2=43$. Nevertheless, this rather naive variational formula provides a simple explanation of the transition with the change of vorticity in the giant vortex. It is interesting to note that due to a logarithmic term, Eq. (7) for the free energy is similar to the free energy of the rotating superfluid

liquid.¹¹ This similarity appears because $\lambda > a$ and all integrals are cut at a , rather than at λ . Moreover, Eq. (7) yields a previously derived estimate for H_{c1} ,⁵ which represents the field at which the first vortex appears in the sample. Substituting $m=1$ into Eq. (1) and solving the equation $F(m=1)=0$ we obtain

$$H_{c1} = \frac{\Phi_0}{2a^2} \cdot \ln(a^2/\pi\xi^2). \quad (9)$$

Note that this expression is similar to the expression for bulk H_{c1} (Ref. 3) where λ^2 is replaced by a^2/π .

In conclusion we have solved the GLE in the limit of $\kappa \rightarrow \infty$ for a thin square film. We have predicted a series of first- and second-order phase transitions with a change of temperature and magnetic field. On the basis of the symmetry we constructed a Landau functional for the second-order transitions. First-order transitions are described on the basis of variational estimates.

We wish to thank D. Mihailović, V.V. Moshchalkov, L. Bulaevskii, and A.S. Alexandrov for many useful discussions and suggestions. We are also grateful to I. Sega for critically reading the manuscript.

¹L.F. Chibotaru, A. Ceulemans, V. Bruyndoncx, and V.V. Moshchalkov, *Nature (London)* **408**, 833 (2000).

²M.B. Sobnack and F.V. Kusmartsev, *Phys. Rev. Lett.* **86**, 716 (2001).

³A.A. Abrikosov, *Zh. Éksp. Teor. Fiz.* **32**, 1442 (1957).

⁴P.C. Bean and J.B. Livingston, *Phys. Rev. Lett.* **12**, 14 (1964).

⁵A.I. Buzdin and J.P. Brison, *Phys. Lett. A* **196**, 267 (1994).

⁶P.S. Deo, V.A. Schweigert, F.M. Peeters, and A.K. Geim, *Phys. Rev. Lett.* **79**, 4653 (1997).

⁷V.A. Schweigert, F.M. Peeters, and P.S. Deo, *Phys. Rev. Lett.* **81**, 2783 (1998).

⁸V.A. Schweigert and F.M. Peeters, *Phys. Rev. Lett.* **83**, 2409 (1999).

⁹Discrete nonlinear Schrödinger Eq. (4) is similar to the equation describing the Holstein polaron on a lattice. V.V. Kabanov and O.Y. Mashtakov, *Phys. Rev. B* **47**, 6060 (1993).

¹⁰B.J. Baelus and F.M. Peeters, cond-mat/0106601 (unpublished).

¹¹I.M. Khalatnikov, *Introduction to the Theory of Superfluidity* (Nauka, Moscow, 1965); W.F. Vinen, in *Superconductivity*, edited by R.D. Parks (Marcel Dekker, New York, 1969), Vol. 2, p. 1167.